

# Experiment of Frequency Range Dependent TE<sub>10</sub> to TE<sub>20</sub> Mode Converter

Yoshihiro Kokubo, Tadashi Kawai

Graduate School of Engineering, University of Hyogo, Himeji-shi, Hyogo, Japan

Email: kokubo@eng.u-hyogo.ac.jp

**How to cite this paper:** Kokubo, Y. and Kawai, T. (2016) Experiment of Frequency Range Dependent TE<sub>10</sub> to TE<sub>20</sub> Mode Converter. *Journal of Electromagnetic Analysis and Applications*, 8, 173-181.

<http://dx.doi.org/10.4236/jemaa.2016.89017>

**Received:** August 4, 2016

**Accepted:** August 30, 2016

**Published:** September 2, 2016

Copyright © 2016 by authors and Scientific Research Publishing Inc.

This work is licensed under the Creative Commons Attribution International

License (CC BY 4.0).

<http://creativecommons.org/licenses/by/4.0/>



Open Access

---

## Abstract

Typical metallic waveguide mode converters convert electromagnetic waves from one mode to another mode for some frequency ranges. However, most electromagnetic waves outside of the specified frequency range are reflected. We report a design for a mode converter which passes the TE<sub>10</sub> mode at a low frequency range and efficiently converts the TE<sub>10</sub> mode to the TE<sub>20</sub> mode at a high frequency range. To gradually shift the mode profile from TE<sub>10</sub> to TE<sub>20</sub>, dielectric rods are placed in a sequence along the waveguide starting near the sidewall and moving to the center of the waveguide with decreasing radius of the rods. This design reduces reflection of electromagnetic waves. Experimental tests demonstrate the efficacy of the design.

## Keywords

Waveguides, Dielectric Array, Scattering Parameter, Mode Converter

---

## 1. Introduction

We have reported that single-mode propagation is available for a metallic waveguide with dielectric rods arrayed at the center of the waveguide in the frequency under twice the cutoff frequency region using the TE<sub>10</sub> mode, and in the frequency over twice the cutoff frequency region using the TE<sub>20</sub> mode, because of restrictions of the TE<sub>10</sub> mode [1] [2]. However, a TE<sub>20</sub>-like mode, which is propagated in the 2nd band, is an odd mode, and generation systems for odd modes have seldom been reported.

In this investigation, we fabricate a mode converter, which passes through the TE<sub>10</sub> mode for the low frequency range and efficiently converts TE<sub>10</sub> to TE<sub>20</sub> mode (or TE<sub>20</sub> to TE<sub>10</sub> mode) for the high frequency range. Typical metallic waveguide mode converters convert electromagnetic waves from one mode to another mode for some frequency range. However, most electromagnetic waves outside of the specified frequency range are reflected [3] [4].

In a rectangular metallic waveguide, only the TE<sub>10</sub> mode propagates for  $0.5 < \omega w/2\pi c < 1$  (the 1st band) for a given frequency  $\omega$ , which is normalized using the width of the waveguide  $w$ . On the other hand, both the TE<sub>10</sub> and TE<sub>20</sub> modes can propagate for  $1 < \omega w/2\pi c < 1.5$  (the 2nd band), where  $c$  is the velocity of light in a vacuum. The TE<sub>10</sub> and TE<sub>20</sub> modes have the same frequency  $\omega$ , but different wave vectors  $k$  and group velocity  $v_g = (dk/d\omega)^{-1}$ . When a mode in the 2nd band is converted from TE<sub>10</sub> to TE<sub>20</sub>, the group velocity of the electromagnetic wave changes. In the 1st band, it cannot be changed.

We have previously reported a waveguide which restricts certain modes [5] and a prototype mode converter [6]. These devices consist of periodic dielectric rod arrays in a waveguide similar to that shown in Figure 1. However, it is not easy to determine the group velocity in the waveguide. The propagation modes in a waveguide having in-line dielectric rods with period  $a$  can be calculated using a supercell approach [7] by applying appropriate periodic Bloch conditions at the boundary of the unit cell [8]. When the location of the dielectric rods is fixed at a distance  $d$  from the sidewall, the group velocity  $v_g$  for both the 1st and 2nd bands can be changed by varying the radius  $r$ . However, the group velocities for both bands are changed at the same time and cannot be changed individually. For  $d$  and  $r$  fixed to certain values,  $v_g/c$  can be calculated for the periodic structure of the dielectric rods at a specific frequency [9].

After calculating  $v_g$  with pairs of  $d$  and  $r$ , each pair of  $d$  and  $r$  is combined.

## 2. Initial Design

We consider a metallic waveguide of size  $17.4 \times 8 \text{ mm}^2$  (cutoff frequency  $f_c \approx 8.62 \text{ GHz}$ ). The period  $a$  is fixed at  $7.2 \text{ mm}$  for target frequencies of  $10 \text{ GHz}$  (1st band) and  $20 \text{ GHz}$  (2nd band). Figure 2 shows a sample of the calculated normalized velocities along the axis of the waveguide at  $10 \text{ GHz}$  and  $20 \text{ GHz}$  for dielectric rods (LaAlO<sub>3</sub>;  $\epsilon_r = 24$ , radius  $r$  (mm)) aligned at a distance from the sidewall  $d$  (mm). It is desirable that the normalized velocity  $v_g/c = 0.902$  (TE<sub>10</sub>: point A) monotonically decrease to  $v_g/c = 0.507$  (TE<sub>20</sub>: point B) at  $20 \text{ GHz}$ , and that the normalized velocity  $v_g/c = 0.507$  (TE<sub>10</sub>: point C) be unchanged at  $10 \text{ GHz}$ . However, at  $20 \text{ GHz}$ , such a condition is not found around  $d = 6 - 7 \text{ mm}$ , because the placement of the dielectric rods at the center of the waveguide minimizes the electric field. On the other hand, placing the dielectric rods near the sidewall of the waveguide maximizes the electric field. At the transition region, around  $d = 6 - 7 \text{ mm}$ , the characteristics are complex. A priority of the design is that the

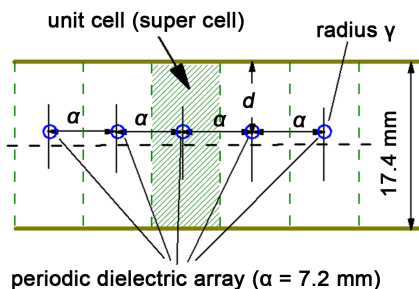
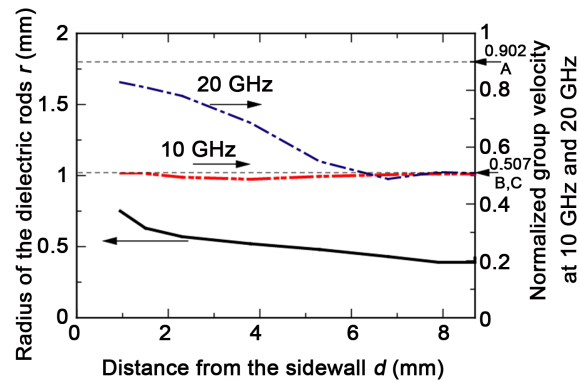


Figure 1. Metallic waveguide with in-line dielectric rods.



**Figure 2.** Group velocity in a metallic waveguide with a periodic array of dielectric rods for various distances from the sidewall  $d$  and various radii of the rods  $r$ , at 20 and 10 GHz.

group velocity at 10 GHz not change. Since the group velocity decreases for dielectric material at 10 GHz and becomes slowest at  $d = 3$  mm, the design employs the 20 GHz frequency for mode conversion, because both the 20 GHz and 10 GHz conditions cannot be satisfied at the same time.

**Figure 3** shows the layout of the rods (though note that rods 0 and 10 are not included in the prototype, but are additions, as detailed below). Since the mode profile gradually shifts from  $TE_{10}$  to  $TE_{20}$ , the dielectric rods are placed progressively away from near the sidewall to the center of the waveguide, as illustrated in the figure. The nine dielectric rods ( $i = 1$  to 9) have decreasing radii  $r_i$  and are placed constant distance apart  $a = 7.2$  mm. Three dielectric rods ( $i = 7, 8,$  and  $9$ ) are located at the center of the waveguide. **Table 1** shows distances  $d_i$  and radii  $r_i$  of the rods.

The S parameters between the input port (Port 1) and output port (Port 2) are calculated using the HFSS software by Ansys [10], and the results are shown as dotted lines in **Figure 4**. The electromagnetic waves enter as the  $TE_{10}$  mode for 9.1 - 14.4 GHz and are converted to the  $TE_{20}$  mode with 18.3 - 21.0 GHz with over 95% efficiency. However, reflection of the  $TE_{10}$  mode at low frequencies and the  $TE_{20}$  mode at high frequencies range are significant under  $-15$  dB, and optimization of the design is necessary to reduce reflection.

### 3. Decreasing the Reflection [9]

As shown in **Figure 4**, the reflection of the  $TE_{10}$  mode is significant around 10 to 14 GHz. This is because the rods located at the center of the waveguide are truncated at Port 2. Another dielectric rod located at the center of the waveguide (rod 10) is needed to decrease electromagnetic reflection. The rod has a smaller cross-section radius of  $r = 0.29$  mm compared with rods 8 and 9. The reflection of the  $TE_{20}$  mode is also significant around 18 to 20 GHz. This is because the rods are located asymmetrically at Port 1. To decrease reflection of the  $TE_{20}$  mode, another dielectric rod (rod 0) is placed on the opposite side of rod 1. The structure of the final design is shown in **Figure 3**. Rods 0 and 10, whose dimensions and locations are shown in **Table 1**, have been added to the structure.

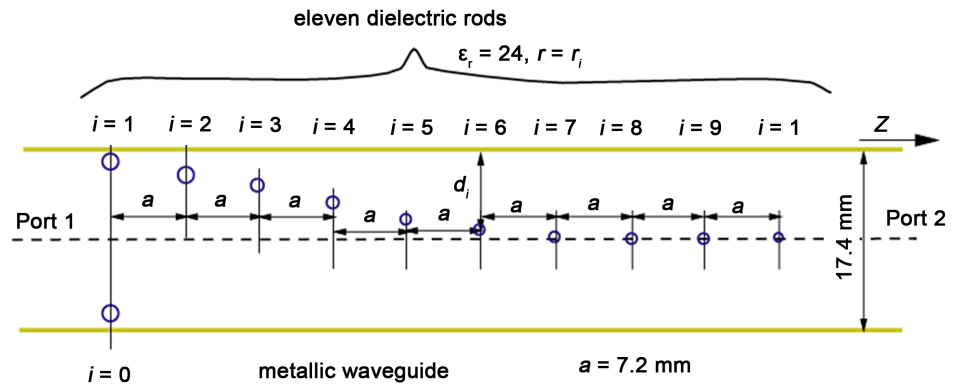


**Figure 3.** Proposed structure of the TE<sub>10</sub> to TE<sub>20</sub> mode converter (the prototype structure does not have rod 0 ( $i = 0$ ) and rod 10 ( $i = 10$ )).

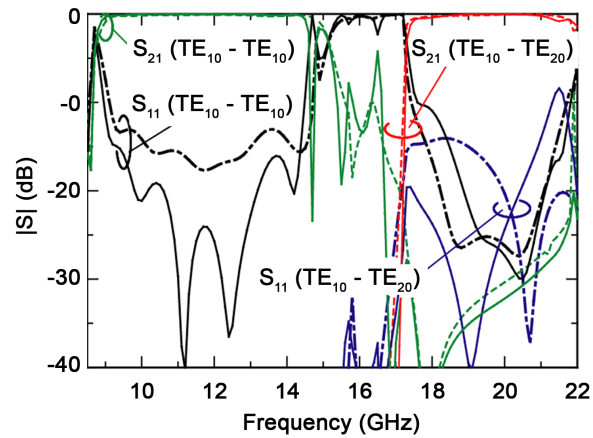


**Figure 4.** S parameters for the mode converter,  $|S_{21}|$  and  $|S_{11}|$  (the dotted lines show the case without rods 0 and 10. The solid lines are for the case with rods 0 and 10.).

**Table 1.** Location and radii of the dielectric rods.

Rod Number $i$	Distance $d_i$ from the Sidewall to the Center of the Rods [mm]	Radius $r_i$ of the dielectric rod [mm]
(0)	(16.45)	(0.73)
1	0.95	0.70
2	2.3	0.57
3	3.8	0.52
4	5.3	0.49
5	6.8	0.43
6	7.9	0.39
7	8.7	0.39
8	8.7	0.42
9	8.7	0.42
(10)	(8.7)	(0.29)

The S parameters between the input port (Port 1) and output port (Port 2) calculated using the HFSS are shown as solid lines in **Figure 4**.

#### 4. Fabrication and Experimental Results

In fabricating a mode converter, such as the Type A illustrated in **Figure 5(a)**, it is necessary to install the dielectric rods in the waveguide without a gap at the top or bottom. Such a structure can be difficult to fabricate. In our approach, holes are machined at the top of the waveguide and the dielectric rods are inserted. For low-cost fabrication, a rectangular dielectric rod quarried from a slab is more suitable than a column (Type B; **Figure 5(b)**). The rectangular dielectric rods are fabricated from slabs of  $\text{LaAlO}_3$  with thicknesses of 0.5, 1.0, and 1.5 mm, and are cut to give cross sections the same as would be the case for columns. The dimensions of the dielectric rectangular rods are shown in **Table 2**.

A problem arises in that a typical coaxial-waveguide converter cannot detect the  $\text{TE}_{20}$  mode since an electrode is placed at the center of the waveguide. Our procedure to detect the  $\text{TE}_{20}$  mode is to first confirm that the  $\text{TE}_{10}$  mode does not propagate to the

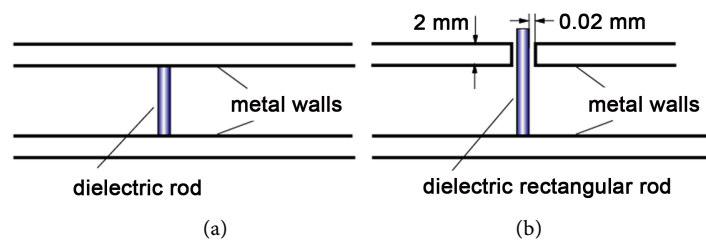


**Figure 5.** (a) Dielectric rod located in a waveguide without gaps at top and bottom; (b) Dielectric rectangular rod inserted in a hole made at the top of the waveguide with a space of 0.02 mm between the rods and the top wall of the waveguide. (a) Type A; (b) Type B.

**Table 2.** Locations and sizes of the dielectric rods arranged in Type B.

Rod Number $i$	Distance $d_i$ from the Sidewall to the Center of the Rectangular Rods [mm]	Length $\times$ Width of the dielectric rod [mm $\times$ mm] (measured value)
0	16.45	1.08 $\times$ 1.553
1	0.95	0.99 $\times$ 1.553
2	2.3	1.026 $\times$ 1.0
3	3.8	1.026 $\times$ 0.74
4	5.3	1.026 $\times$ 0.57
5	6.8	0.524 $\times$ 0.91
6	7.9	0.524 $\times$ 0.91
7	8.7	0.524 $\times$ 0.91
8	8.7	0.524 $\times$ 1.06
9	8.7	0.524 $\times$ 1.06
10	8.7	0.524 $\times$ 0.50

end of the  $TE_{10}$  to  $TE_{20}$  mode converter at mode conversion frequency and then to connect another mode converter of the same type to the original converter in the opposite direction and measure the reconverted  $TE_{10}$  from  $TE_{20}$  mode.

Fabricated mode converters have a full length of 130 mm. The outside appearance is shown in **Figure 6** and the experimental setups are shown in **Figures 7(a)-(c)**. **Figure 7(a)** is the setup for confirming that the  $TE_{10}$  mode has passed through the mode converter at the low frequency range. The mode converter was connected to a HP-8510B

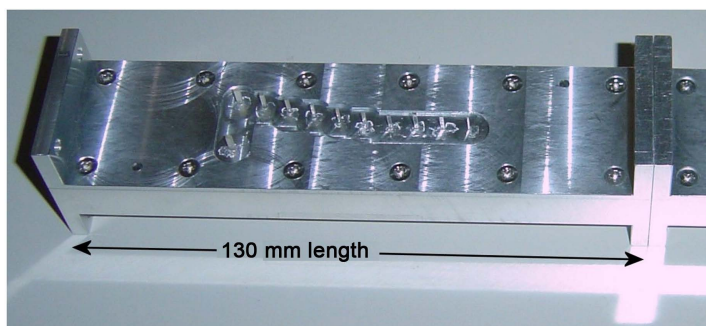


**Figure 6.** Frequency range dependent mode converter.

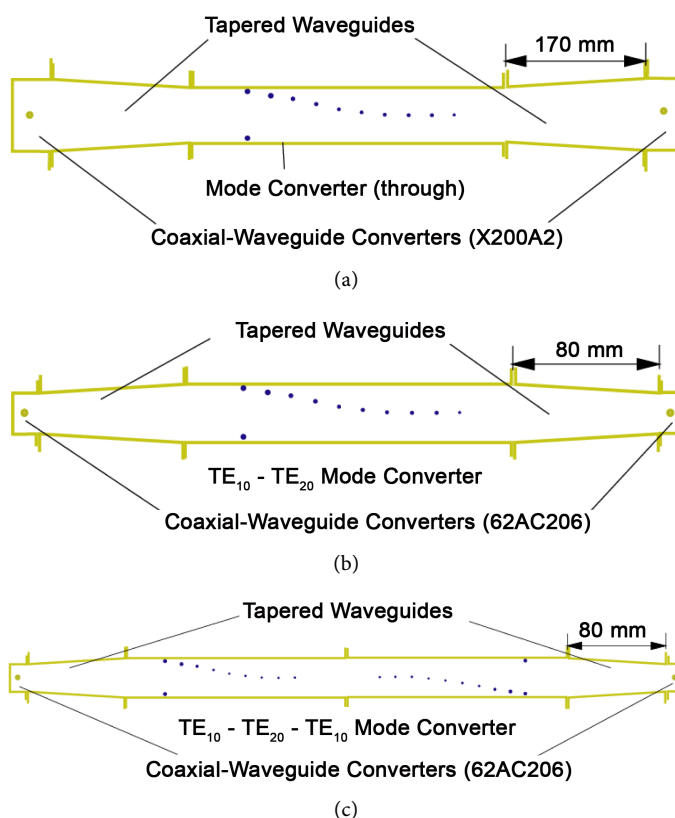
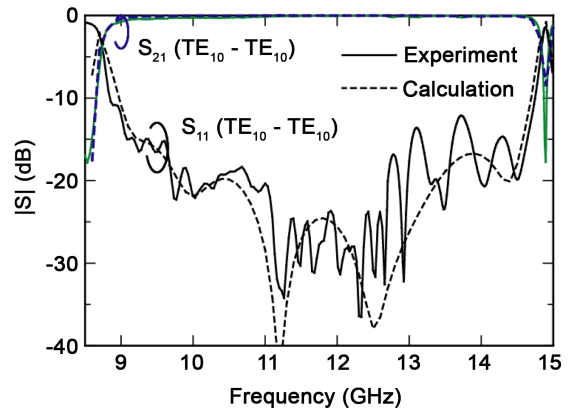


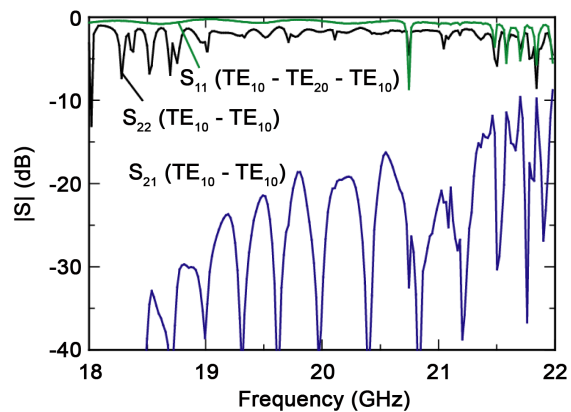
**Figure 7.** Experimental setup for measurement of S parameters. (a)  $|S_{21}|$  and  $|S_{11}|$  at low frequencies; (b)  $|S_{21}|$  ( $TE_{10} - TE_{10}$ ),  $|S_{11}|$  ( $TE_{10} - TE_{20} - TE_{10}$ ) and  $|S_{22}|$  ( $TE_{10} - TE_{10}$ ) at high frequencies. (c)  $|S_{21}|$  ( $TE_{10} - TE_{20} - TE_{10}$ ) and  $|S_{11}|$  ( $TE_{10} - TE_{10}$ ,  $TE_{10} - TE_{20} - TE_{10}$  and  $TE_{10} - TE_{20} - TE_{10} - TE_{10}$ ).

network analyzer by a coaxial-waveguide converter (Maury Microwave X200A2: 8.2 - 12.4 GHz, VSWR max = 1.05) through a tapered waveguide of 170 mm length.

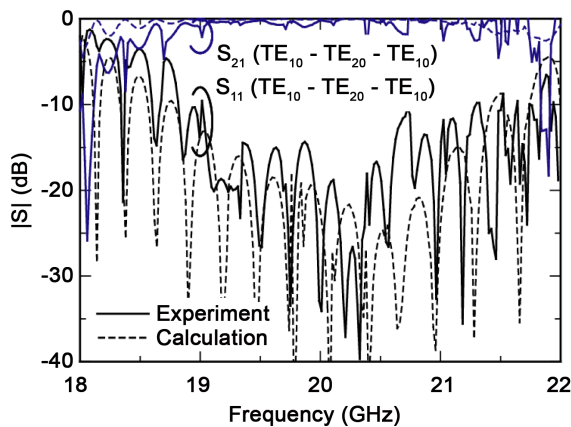
The experimental results are shown in **Figure 8(a)** as solid lines. The dotted lines indicate the calculated results and are sufficiently consistent with the experimental re-



(a)



(b)



(c)

**Figure 8.** Experiment results of S parameters: (a)  $|S_{21}|$  and  $|S_{11}|$  in **Figure 7(a)**; (b)  $|S_{21}|$ ,  $|S_{11}|$  and  $|S_{22}|$  in **Figure 7(b)**; (c)  $|S_{21}|$  and  $|S_{11}|$  in **Figure 7(c)**.

sults. **Figure 7(b)** is the setup for confirming that the  $TE_{10}$  mode is converted to the  $TE_{20}$  and that the  $TE_{10}$  is not propagated (the coaxial-waveguide converter is a Fairview Microwave Inc. 62AC206: 12.4 - 18.0 GHz, VSWR max = 1.25). The experimental results are shown in **Figure 8(b)** as solid lines. The figures show that  $S_{21}$  for the  $TE_{10}$  mode propagation is very small.

To measure the conversion efficiency from the  $TE_{10}$  to  $TE_{20}$  mode, another of the same type of mode converter is connected in the opposite direction to the previous mode converter. The values of the S parameter  $S_{21}$  is the conversion efficiency after converting from  $TE_{10}$  to  $TE_{20}$  and reconverting from  $TE_{20}$  to  $TE_{10}$ . **Figure 8(c)** shows the experimental results for the setup shown in **Figure 7(c)**. The solid lines are experimental results and are almost the same as the calculation results shown as dotted lines.

## 5. Conclusion

We have proposed a frequency range dependent  $TE_{10}$  to  $TE_{20}$  mode converter that efficiently converts the low frequency  $TE_{10}$  mode to the high frequency  $TE_{20}$  mode by small variations of the group velocity of the  $TE_{10}$  mode. The mode converter allows low frequency electromagnetic waves to pass through but converts higher frequency electromagnetic waves from the  $TE_{10}$  mode to  $TE_{20}$  mode without reflection. We demonstrate that electromagnetic waves pass through in the  $TE_{10}$  mode at 9.7 - 14.6 GHz and are converted to the  $TE_{20}$  mode at 19.1 - 20.3 GHz at over 95% efficiency. Such frequency range dependent mode converters are useful for applications that require single-mode propagation at two frequencies.

## Acknowledgements

The authors thank Mr. H. Miyazaki for help with the experiment set-up.

## References

- [1] Kokubo, Y. (2007) Wide Band Metallic Waveguide with In-Line Dielectric Rods. *IEICE Transactions on Electronics*, **J90-C**, 642-643. (In Japanese)
- [2] Kokubo, Y. and Kawai, T. (2009) 90-Degree H-Plane Bent Waveguide Using Dielectric Rods. *Microwave and Optical Technology Letters*, **51**, 2015-2017. <http://dx.doi.org/10.1002/mop.24573>
- [3] Zhang, Q., Yuan, C.W. and Liu, L. (2012) Theoretical Design and Analysis for  $TE_{20}$ - $TE_{10}$  Rectangular Waveguide Mode Converters. *IEEE Transactions on Microwave Theory and Techniques*, **60**, 1018-1026. <http://dx.doi.org/10.1109/TMTT.2011.2182206>
- [4] Xu, C., Tantawi, S. and Wang, J. (2014) Novel X Band Compact Waveguide Dual Circular Polarizer. Cornell University Library, 1406.7266.
- [5] Kokubo, Y. (2008) Wide Band Metallic Waveguide with In-Line Dielectric Rods. *IEEE Microwave and Wireless Components Letters*, **18**, 79-81. <http://dx.doi.org/10.1109/LMWC.2007.915028>
- [6] Kokubo, Y. (2010) Frequency Range Dependent  $TE_{10}$  to  $TE_{20}$  Mode Converter. *Microwave and Optical Technology Letters*, **52**, 169-171. <http://dx.doi.org/10.1002/mop.24886>
- [7] Benisty, H. (1996) Modal Analysis of Optical Guides with Two-Dimensional Photonic

Band-Gap Boundaries. *Journal of Applied Physics*, **79**, 7483-7492.

<http://dx.doi.org/10.1063/1.362419>

- [8] Boroditsky, M., Coccioli, R. and Yablonovitch, E. (1998) Analysis of Photonic Crystals for Light Emitting Diodes Using the Finite Difference Time Domain Technique. *Proceedings of SPIE*, **3283**, 184-190. <http://dx.doi.org/10.1117/12.316682>
- [9] Kokubo, Y. (2011) Waveguide Mode Converters. Chapter 14, *Electromagnetic Waves/Book 1*, In-Tech, Vienna, 283-296. <http://dx.doi.org/10.5772/16609>
- [10] Ansys, Inc. (2007) Achieve High-Frequency, High-Speed Component Design Tools from ANSYS. HFSS V11.



Scientific Research Publishing

**Submit or recommend next manuscript to SCIRP and we will provide best service for you:**

Accepting pre-submission inquiries through Email, Facebook, LinkedIn, Twitter, etc.

A wide selection of journals (inclusive of 9 subjects, more than 200 journals)

Providing 24-hour high-quality service

User-friendly online submission system

Fair and swift peer-review system

Efficient typesetting and proofreading procedure

Display of the result of downloads and visits, as well as the number of cited articles

Maximum dissemination of your research work

Submit your manuscript at: <http://papersubmission.scirp.org/>